Available online at www.sciencedirect.com
SCIENCE DIRECT
Journal of Magnetic Resonance 181 (2006) 29–34
JMR Journal of Magnetic Resonance
www.elsevier.com/locate/jmr

Thermal diffusivity and nuclear spin relaxation: A continuous wave free precession NMR study

Tiago Venâncio [a,b], Mario Engelsberg [c], Rodrigo B.V. Azeredo [d], Luiz A. Colnago [b,*]

[a] Universidade de São Paulo, Instituto de Química de São Carlos, Avenida Trabalhador São-Carlense 400, São Carlos, SP 13560-590, Brazil
[b] Embrapa Instrumentação Agropecuária, Rua 15 de Novembro 1452, São Carlos, SP 13560-970, Brazil
[c] Universidade Federal de Pernambuco, Departamento de Física, Avenida Professor Luiz Freire s/n° Cidade Universitária, Recife, PE 50670-901, Brazil
[d] Universidade Federal Fluminense, Instituto de Química, Outeiro de São João Batista s/n°, Campus do Valonguinho, Niterói, RJ 24020-150, Brazil

Received 12 December 2005; revised 8 March 2006
Available online 17 April 2006

Abstract

Continuous wave free precession (CWFP) nuclear magnetic resonance is capable of yielding quantitative and easily obtainable information concerning the kinetics of processes that change the relaxation rates of the nuclear spins through the action of some external agent. In the present application, heat flow from a natural rubber sample to a liquid nitrogen thermal bath caused a large temperature gradient leading to a non-equilibrium temperature distribution. The ensuing local changes in the relaxation rates could be monitored by the decay of the CWFP signals and, from the decays, it was possible to ascertain the prevalence of a diffusive process and to obtain an average value for the thermal diffusivity.

Keywords: Thermal diffusivity; Natural polymer; CWFP; SSFP; Freezing

1. Introduction

Steady-state free precession (SSFP) [1–4] has been very effective in fast magnetic resonance imaging and in the study of flow and diffusion [5–7]. Recently, we have demonstrated that continuous wave free precession (CWFP), a special case of SSFP, can be used in several applications. For example: for signal to noise ratio improvement in quantitative determinations using low-resolution NMR equipment [8,9], to monitor flow [10], and for fast simultaneous measurements of T_1 and T_2 [11].

The CWFP regime is attained when a train of short $\pi/2$ pulses, with period T_p small compared to $T_2^* = 1/\Delta\varpi_0$, is applied to a liquid or motionally narrowed solid obeying Bloch's equations. Here $\Delta\varpi_0$ denotes the dispersion of precession frequencies about a central frequency ϖ_0 caused by an inhomogeneous magnetic field. Furthermore, the applied radiofrequency is shifted from the central frequency ϖ_0 by a frequency offset chosen such that $\omega_0 T_p = (2n+1)\pi$, where n is an integer. This causes the signal amplitude just preceding a $\pi/2$ pulse to be equal to the amplitude following the pulse. Since the condition $T_p < T_2^*$ implies that dephasing of isochromats in each interval T_p is relatively small a continuous wave periodic signal with practically constant amplitude, displaying n nodes within each T_p interval, is obtained [8]. If the condition $T_p \ll T_2$, T_1 is satisfied the amplitude of the transverse CWFP magnetization, under steady-state conditions, can be shown to be given by [8] $|M_{s+}| = M_0/(1 + T_1/T_2)$. Here T_2 is the spin–spin relaxation time and M_0 denotes the thermal equilibrium magnetization.

When a CWFP steady state is established under equilibrium conditions its amplitude is determined by the time-independent ratio $\Gamma = T_1/T_2$. Moreover, in a non-equilibrium situation, the steady-state signal can evolve in time as changes in the relaxation times, which could be caused by a variety of processes, take place. Such processes might include: temperature changes due to heat transfer,

* Corresponding author. Fax: +55 1633725958.
E-mail address: colnago@cnpdia.embrapa.br (L.A. Colnago).

1090-7807/$ - see front matter © 2006 Elsevier Inc. All rights reserved.
doi:10.1016/j.jmr.2006.03.011

fast polymerization reactions, phase changes, etc. Provided the response of the CWFP signal is fast enough, valuable information about the kinetics of these processes could be obtained.

CWFP can be used effectively to monitor such processes provided some specific conditions are met. Denoting by τ the correlation time of the relevant molecular motion CWFP can be sensitive to the kinetics of the process provided the motion is in the slow correlation time regime [12] characterized by $\varpi_0\tau > 1$. In this regime, the spin–lattice relaxation time can become appreciably longer than the spin–spin relaxation time. Conversely, in extreme narrowing regime characterized by $\varpi_0\tau \ll 1$, the condition $T_1 \approx T_2$ prevails and the CWFP signal becomes independent of the relaxation times.

The response time of the CWFP signal to changes in the relaxation times is an important factor for the proposed application. The establishment of a steady-state CWFP signal starting from thermal equilibrium has been studied in considerable detail. It has been shown to consist of an initial oscillatory transient [11], with a short time constant determined by T_2^* superimposed on an exponential approach to the steady state with time constant [13] $T_s = 2T_1T_2/(T_1 + T_2)$. One could expect that, if the rate of change of the relaxation ratio $\Gamma = T_1/T_2$ for the ongoing process is smaller than $1/T_s$ the CWFP signal should be able to follow the kinetics of the process. In a regime characterized by $\varpi_0\tau > 1$ the spin–lattice relaxation time T_1 may become quite longer than T_2 and the response time approaches the value $T_s \approx 2T_2$.

Although several applications can be conceived we here consider, as an example, the heat transport process in spheres of a polyisoprene elastomer (natural unvulcanized latex rubber without any filler). In spite of being able, in principle, to monitor faster processes, there exists some interest in measuring thermal transport properties by NMR [14–16].

Starting from a spatially non-uniform temperature distribution the system under study, with a well-defined geometrical shape, is allowed to evolve towards equilibrium via thermal diffusion. As the local temperature varies the changes in ^{1}H relaxation times that take place can be monitored through the decay of the CWFP signal. By varying the size of the system it is possible to make sure that the scaling of the decays obeys a diffusion equation and to ascertain that the response time comfortably permits to monitor the kinetics of the process.

Using low-resolution bench-top NMR equipment, and combining CWFP measurements under non-equilibrium conditions with equilibrium CWFP measurements at various temperatures, we are able to obtain thermal diffusivity data.

2. Theory

In several elastomers, such as natural rubber, at Larmor frequencies in the range $\varpi_0/2\pi \sim 5$ MHz, the condition $\varpi_0\tau > 1$ is satisfied for T_1 somewhat below room temperature. Here τ represents the correlation time of the motion, which in the present case, corresponds to the reorientation of elementary polymer segments.

If a uniform polymer sample of spherical shape, initially in equilibrium at a temperature θ_0, is placed in contact with a thermal bath at a lower temperature θ_b, the time evolution of the local temperature $\Theta(r,t)$ resulting from heat flow to the bath can be described by a diffusion equation. For spherical symmetry the local temperature $\Theta(r,t)$ obeys the equation

$$\frac{\partial\Theta}{\partial t} = \frac{1}{r^2}\frac{\partial}{\partial r}\left(\lambda(\Theta)r^2\frac{\partial\Theta}{\partial r}\right), \tag{1}$$

where the thermal diffusivity $\lambda(\Theta)$ is, in general, a function of temperature and is related to the heat conductivity κ, the specific heat at constant pressure c_p, and the mass density ρ through [17]

$$\lambda = \frac{\kappa}{c_p\rho}. \tag{2}$$

In particular, if the thermal diffusivity can be assumed to be temperature independent in the interval of interest, the diffusion equation takes the simpler form

$$\frac{\partial\Theta}{\partial t} = \frac{\lambda}{r}\frac{\partial^2}{\partial r^2}(r\Theta). \tag{3}$$

Denoting by a the radius of the sphere, Eq. (3) permits an analytical solution [17], satisfying the boundary conditions of our problem, which is given in closed form by

$$\frac{\Theta(r,t) - \theta_0}{\theta_b - \theta_0} = 1 + 2\sum_{n=1}^{\infty}(-1)^n \exp(-n^2\lambda\pi^2 t/a^2)\frac{\sin(\pi nr/a)}{\pi nr/a}, \tag{4}$$

in the range $t > 0$ and $r < a$.

On the other hand, when the thermal diffusivity changes appreciably in the temperature interval of interest, Eq. (2) can be solved numerically using, for example, the finite differences method of Crank–Nicholson [17,18] with a temperature dependent $\lambda(\Theta)$.

As the local temperature within the sphere decreases from its initial uniform value θ_0 towards its final equilibrium value θ_b the relaxation ratio $\Gamma = T_1/T_2$ rapidly increases and the CWFP signal amplitude decays to zero. Strictly speaking not only the relaxation ratio increases but also the thermal equilibrium magnetization increases at a rate limited by $1/T_1$. However, given that the changes in M_0 are small in the present problem, the effect is practically negligible.

If the rate of change of the ratio T_1/T_2 is small compared with $1/T_s$ the CWFP signal amplitude as a function of time can be assumed to be determined by the time evolution of a succession of steady-state regimes. Denoting by $\Gamma(\Theta) = T_1(\Theta)/T_2(\Theta)$ the temperature-dependent relaxation ratio, the normalized CWFP signal amplitude $S(t)$ would be given simply by an integral over all spherical shells of form

$$S(t) = \frac{(1+\Gamma(\theta_0))}{(4/3)\pi a^3}\int_0^a \frac{4\pi r^2\,\mathrm{d}r}{1+\Gamma(\Theta(r,t))}. \quad (5)$$

The correction arising from the variation of M_0 with temperature, as predicted by Curie's law, can be taken into account by multiplying the integrand in Eq. (5) by $\theta_0/\Theta(r,t)$. However, given the steep variation with temperature of the relaxation ratio $\Gamma(\Theta)$, the resulting correction is quite small.

Eq. (5) can be used to determine the average thermal diffusivity of the polymeric material. First the functional form of $\Gamma(\Theta)$ must be determined experimentally by measuring the relaxation ratio Γ at various temperatures. A simple way to do that is to measure the ratio $|M_{s+}|/M_0$ for the polymer in equilibrium at various temperatures directly from the CWFP signal amplitude. Moreover, since the functional dependence $\Theta(r,t)$ is furnished by the solution of the diffusion equation it is possible, using Eq. (5), to calculate the time dependence of the CWFP signal decay under non-equilibrium conditions.

3. Experimental results and discussion

^{1}H CWFP measurements were performed at a frequency of 7.24 MHz using a home-made [8] system with a bench-top 0.17 T Alnico V permanent magnet. The dephasing caused by the inhomogeneity of the magnetic field could be characterized by a characteristic time $T_2^* = 1.0$ ms and the period of the sequence of $\pi/2$ pulses was $T_p = 0.3$ ms. The frequency offset, $\Delta = \varpi - \omega_0$, was chosen such that $\Delta T_p = 3\pi$ and the width of a $\pi/2$ pulse was 9 μs. Pulse imperfections can have some effect on the CWFP signal amplitude, as demonstrated in [11]. Good homogeneity of the RF field over the volume sample volume is generally necessary but the required conditions can be met without great difficulty.

The probe consisted of a single receive/transmit coil 25 mm in diameter and 25 mm in height and the electronic hardware consisted of a Apollo transceiver (Tecmag) used in conjunction with a Miteq AU1448 preamplifier and a AMT2053 power amplifier.

The rubber spheres were introduced in a glass tube 23 mm in diameter and 200 mm in height which was not in direct contact with the RF coil. A steady-state CWFP regime was first established at $\theta_0 = 295$ K by applying a train of $\pi/2$ pulses for approximately 3 s. At this point a non-equilibrium initial condition was created by establishing contact between the rubber spheres and a liquid nitrogen bath at temperature $\theta_b = 77.8$ K. Liquid nitrogen was poured on the samples, keeping the spheres immerse, while signal acquisition was started simultaneously with the addition of the liquid nitrogen. Initial boil-off instabilities appeared to have little effect on the CWFP signal. Furthermore, detuning and mismatching caused by the addition of liquid nitrogen was also found to be negligible. The CWFP pulse sequence applied in this experiment consisted of a train of 9×10^4 pulses separated by a time interval T_p of 300 μs.

Bath temperatures closer to θ_0 could yield more accurate thermal diffusivity data but, since longer decays would prevail, the time response of the CWFP method would not be adequately tested.

Fig. 1 shows CWFP signal decays for spherical samples of various masses. Each of the 10K data points in every decay was acquired at $9T_p$ intervals (2.7 ms) and corresponds to an average of 64 points sampled with a dwell time of 4 μs.

Fig. 1 shows various decays in spheres of different masses, indicating that the decay rates increase as the mass of the spheres decreases. This can be seen more clearly in Fig. 2 where normalized decays have been plotted. The decay of Fig. 1 corresponding to a mass of 0.47 g, with

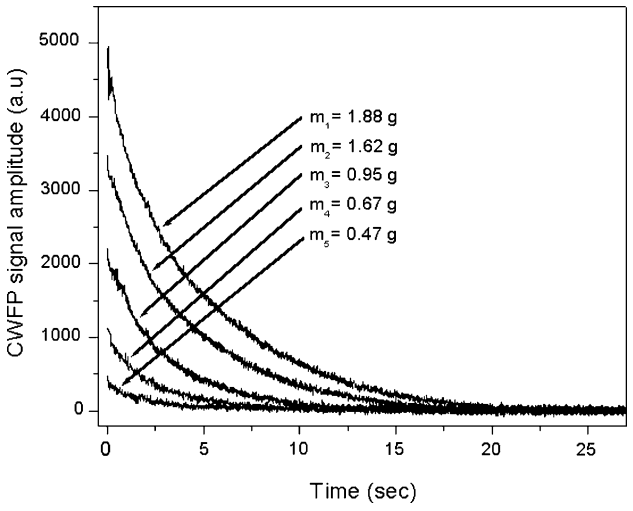

Fig. 1. CWFP signal amplitude decays for rubber spheres of various masses, initially at $\theta_0 = 295$ K, after contact with a bath at $\theta_b = 77.8$ K.

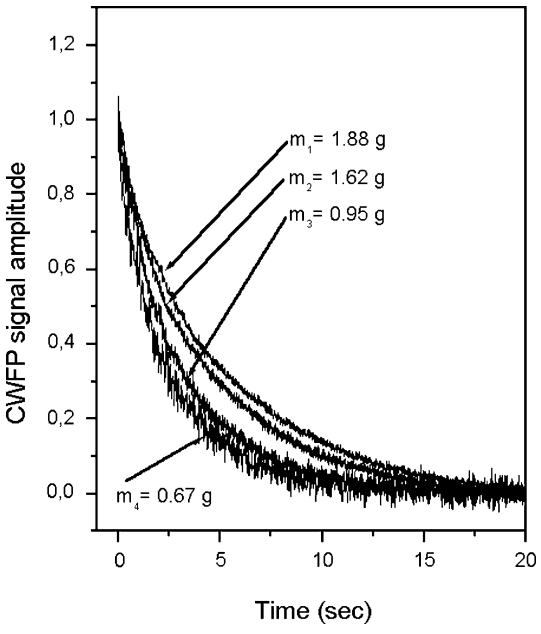

Fig. 2. Normalized CWFP signal decays for rubber spheres with four different masses.

relatively poor signal to noise ratio, has been removed from Fig. 2 to improve clarity.

According to Eq. (4), and also from the more general Eq. (1), the time dependence of the decays of Fig. 2 should be governed by the variable t/a^2. Hence, if one neglects variations in the mass density ρ, and the data of Fig. 2 are plotted as a function of the variable t/a^2, one should obtain a universal decay curve. Equivalently, all decays should also collapse into a universal decay if one plots as a function of $t/m^{2/3}$, where m denotes the mass of a sphere and $m^{2/3} = a^2\ (4\pi\rho)^{2/3}$.

Fig. 3 shows a universal decay obtained by plotting each of the four decays of Fig. 2 as a function of $1/m^{2/3}$ which confirms the prediction of the diffusion equation. For the decay corresponding to $m = 0.47$ g, not shown in Fig. 3, the poorer signal to noise ratio only permits to determine the value of the mass exponent as 0.66 ± 0.05.

Given that the decays of Fig. 2 scale with time according to the prediction of the diffusion equation one could now attempt to employ Eq. (5) to fit the universal curve of Fig. 3 by first assuming a constant diffusivity. To that end one needs to first determine the temperature dependence $\Gamma(\Theta)$ of the relaxation ratio. Since the motions relevant for T_1 and T_2 are thermally activated one can expect, in the region $\varpi_0\tau > 1$, a functional dependence of form $\Gamma(\Theta) = \mathrm{A} + \mathrm{B}\exp(E_\Gamma/k_\mathrm{B}\Theta)$, where the exponent E_Γ contains contributions from the motions relevant for T_1 at the given frequency as well as of T_2. Hence the temperature dependence of $\Gamma(\Theta)$ is expected to be, in general, steeper than that of T_1 or T_2.

The parameters A, B, and E_Γ could be determined from measurements of the ratio $|M_{s+}|/M_0$ of the CWFP signal in the steady state to the thermal equilibrium signal amplitude. At a temperature of $\theta_0 = 295$ K values of $T_1 = 13$ ms and $T_2 = 5.5$ ms were independently measured by inversion recovery [19] and Carr–Purcell–Meiboom–Gill [20] sequences respectively, yielding a ratio $\Gamma(\theta_0) = 2.36$ for $\varpi_0/2\pi = 7.24$ MHz.

Fig. 4 shows measurements of the relaxation ratio Γ as a function of $1/\Theta$ obtained from CWFP measurements in rubber at various temperatures under thermal equilibrium conditions. For temperatures below the T_1 minimum at $\Theta \approx 298$ K the ratio $\Gamma(\Theta)$ rises quite steeply and the CWFP signal amplitude $|M_{s+}|/M_0 = 1/(1 + \Gamma(\Theta))$ reaches noise level at $\Theta \approx 268$ K. Hence, only spins in a relatively narrow temperature range below θ_0 are effectively involved in the decays of Fig. 1. From a best fit to the data of Fig. 4 one obtains $A = 1.846$, $E_\Gamma/k_\mathrm{B} = 5600$ K, and $B = 0.607 \times 10^{-8}$. It is worth pointing out that for $\varpi_0/2\pi = 5$ MHz the spin–lattice relaxation time in polyisoprene [21] exhibits, in the region $\varpi_0\tau > 1$, an exponential growth parameter $E_1/k_\mathrm{B} \approx 3775$ K, considerably smaller than E_Γ/k_B.

It is now possible to employ Eqs. (4) and (5) to calculate the universal decay curve and obtain an average value $\bar{\lambda}$ of the thermal diffusivity in the interval θ_0 to θ_b from an adjustment to the data of Fig. 3. Fig. 5 shows the theoretical decay corresponding to $\bar{\lambda} = 1.684 \times 10^{-3}$ cm^2/s obtained from Eqs. (4) and (5) including the small Curie law correction.

Given the simple theory employed and the approximations involved, the overall agreement is quite rewarding. Deviations from spherical shape in our samples as well as density variations with temperature may explain some small but systematic departures in Fig. 5. It is instructive

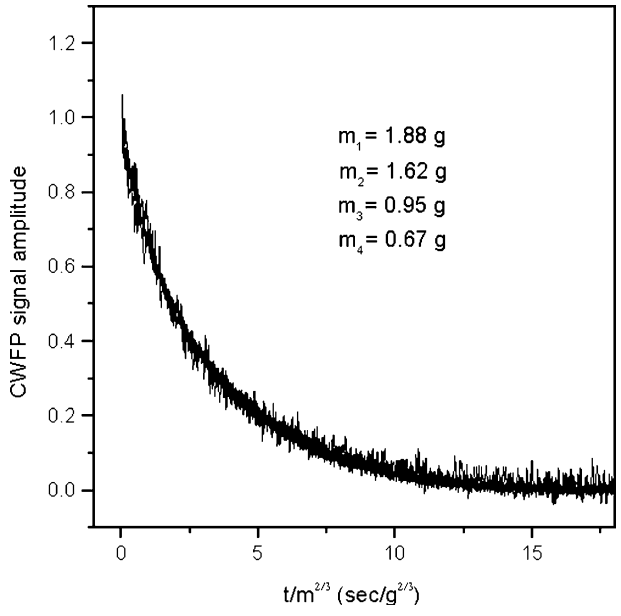

Fig. 3. Universal CWFP signal decay for rubber spheres with four different masses obtained by plotting as a function the scaled time variable $t/m^{2/3}$.

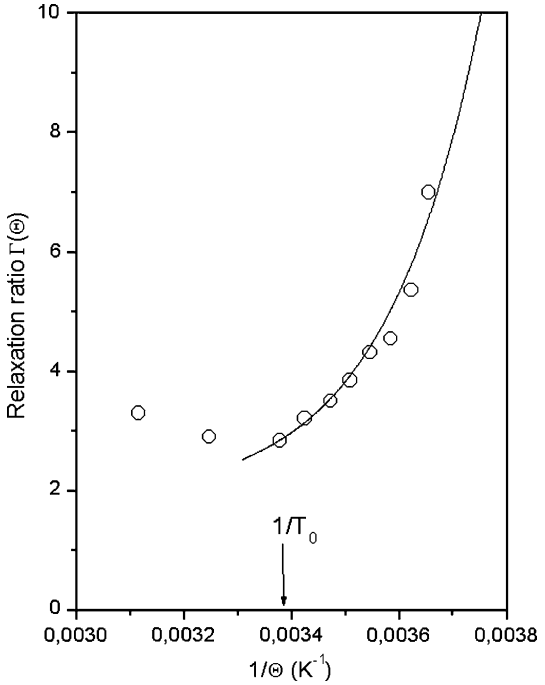

Fig. 4. Relaxation ratio $\Gamma(\Theta)$ as a function of inverse temperature $1/\Theta$ obtained from CWFP steady-state signal amplitudes in thermal equilibrium. The solid line is an empirical fit of the data in the region of interest $\Theta < \theta_0$.

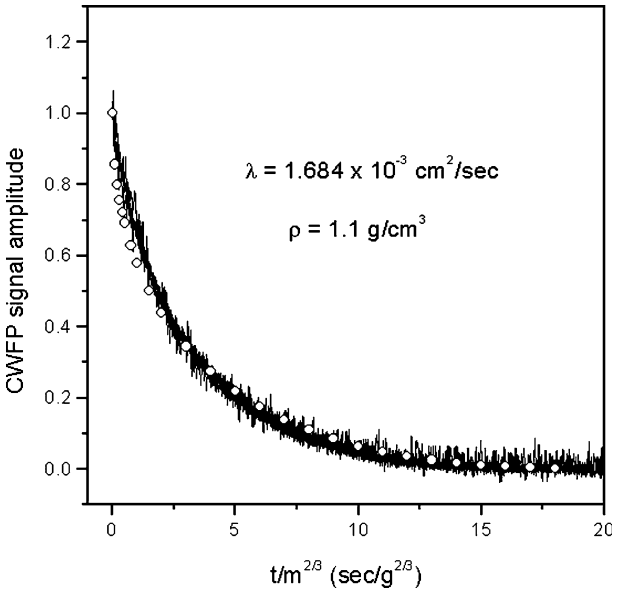

Fig. 5. Universal CWFP decay for rubber spheres. The circles are calculated values assuming an average thermal diffusivity $\bar{\lambda} = 1.684 \times 10^{-3}$ cm^2/s and a constant mass density $\rho = 1.1$ g/cm^3.

to compare the value of $\bar{\lambda}$ obtained from Fig. 5 with values found in the literature for related materials. For vulcanized rubber, for example, the heat conductivity [22] κ and the specific heat at constant pressure[23] c_p have been separately measured in the temperature range $100\ \text{K} < \Theta < 290\ \text{K}$ yielding $\kappa(290\ \text{K}) = 1.36 \times 10^{-3}$ W/cm K and c_p (290 K) ≈ 1.8 J/g K. Assuming $\rho \approx 1.1$ g/cm^3 one obtains from Eq. (2) $\lambda(290\ \text{K}) = 0.69 \times 10^{-3}$ cm^2/s. This value appears to remain approximately constant from 290 K to approximately 200 K and drop rather abruptly below 200 K.

Although the decay rate of the theoretical curve of Fig. 5 is quite sensitive to the value of the average thermal diffusivity $\bar{\lambda}$, its shape alone is not very useful to determine the temperature dependence of the diffusivity. To prove this point, we solved Eq. (1) numerically by the implicit finite difference method of Crank–Nicholson [17,18] assuming, for example, a linear variation with temperature of $\lambda(\Theta)$. The calculations indicated that, after the integration over the sphere implied by Eq. (5), it is possible, for realistic parameters, to find an average constant value $\bar{\lambda}$ that yields essentially the same curve as the linearly temperature dependent $\lambda(\Theta)$. Other monotonic temperature dependences yielded similar conclusions. Thus, if one wishes to extract some information concerning the temperature dependence of $\lambda(\Theta)$ from Fig. 5 it would be necessary to determine thermal diffusivity values at some narrow temperature intervals.

4. Conclusions

We have shown that the CWFP technique is capable of yielding quantitative and easily obtainable information concerning the kinetics of processes that change the relaxation rate of the nuclear spins through the action of some external agent. In this particular application heat flow caused by a large temperature gradient led to local changes in the relaxation rates that could be monitored by the decay of the CWFP signal. From the decays it was possible to ascertain the prevalence of a diffusive process and to obtain an average value for the thermal diffusivity.

Acknowledgments

We thank FAPESP (02/05409-0 and 04/11904-9), CNPq, and FINEP/RBT for support.

References

[1] H.Y. Carr, Steady-state free precession in nuclear magnetic resonance, Phys. Rev. 112 (1958) 1693–1701.
[2] R.R. Ernst, W. Anderson, Application of Fourier transform spectroscopy to magnetic resonance, Rev. Sci. Instrum. 37 (1966) 93–102.
[3] R. Freeman, H.D.W. Hill, Phase and intensity anomalies in Fourier transform NMR, J. Magn. Res. 4 (1971) 366–383.
[4] A. Schwenk, NMR pulse technique with high sensitivity for slowly relaxing systems, J. Magn. Res. 5 (1971) 376–389.
[5] R.C. Hawkes, S. Patz, Rapid Fourier-imaging using steady-state free precession, Magn. Res. Med. 4 (1) (1987) 9–23.
[6] C.E. Carney, S.T.S. Wong, S. Patz, Analytical solution and verification of diffusion effect in SSFP, Magn. Res. Med. 19 (1991) 240–246.
[7] D.E. Freed, U.M. Scheven, L.J. Zielinski, P.N. Sen, M.B. Hürlimann, Steady-state free precession experiments and exact treatment of diffusion in a uniform gradient, J. Chem. Phys. 115 (9) (2001) 4249–4258.
[8] R.B.V. Azeredo, L.A. Colnago, M. Engelsberg, Quantitative analysis using steady-state free precession nuclear magnetic resonance, Anal. Chem. 72 (2000) 2401–2405.
[9] R.B.V. Azeredo, L.A. Colnago, A.A. Souza, M. Engelsberg, Continuous wave free precession—practical analytical tool for low-resolution nuclear magnetic resonance measurements, Anal. Chim. Acta 478 (2003) 313–320.
[10] R.B.V. Azeredo, M. Engelsberg, L.A. Colnago, Flow sensitivity and coherence in steady-state free spin precession, Phys. Rev. E 64 (2001) 016309–016313.
[11] T. Venâncio, M. Engelsberg, R.B.V. Azeredo, N.E.R. Alem, L.A. Colnago, Fast and simultaneous measurement of longitudinal and transverse NMR relaxation times in a single continuous wave free precession experiment, J. Magn. Res. 173 (2005) 34–39.
[12] A. Abragam, Principles of Nuclear Magnetism, International Series of Monographs on Physics, Oxford, 1983.
[13] J. Kronenbitter, A. Schwenk, New technique for measuring relaxation-times T_1 and T_2 and equilibrium magnetization M_0 of slowly relaxing systems with weak NMR signals, J. Magn. Res. 25 (1977) 147–165.
[14] P.S. Belton, Advances in Magnetic Resonance in Food Science, Royal Society of Chemistry, Cambridge, 1999.
[15] W.L. Kerr, R.J. Kauten, M. Ozilgen, M.J. McCarthy, D.S. Reidl, NMR imaging, calorimetric, and mathematical modeling studies of food freezing, J. Food Proc. Eng. 19 (1996) 363–384.
[16] W.L. Kerr, C.J. Clark, M.J. McCarthy, J.S. de Ropp, Freezing effects in fruit tissue of kiwifruit observed by magnetic resonance imaging, Sci. Horticult. 69 (1997) 169–179.
[17] J. Crank, The Mathematics of Diffusion, second ed., Clarendon Press, Oxford, 1986.
[18] A. Mikkelsen, A. Elgsaeter, Density distribution of calcium-induced alginate gels. a numerical study, Biopolymers 36 (1995) 17–41.
[19] (a) R.L. Vold, J.S. Waugh, M.P. Klein, D.E. Phelps, Measurement of spin relaxation in complex systems, J. Chem. Phys. 48 (1968) 3831–3832;

(b) R. Freeman, H.D.W. Hill, High-resolution studies of nuclear spin–lattice relaxation, J. Chem. Phys. 51 (1969) 3140–3141.

[20] (a) H.Y. Carr, E.M. Purcell, Effects of diffusion on free precession in nuclear magnetic resonance experiments, Phys. Rev. 94 (1954) 630–638;
(b) S. Meiboom, D. Gill, Modified spin-echo method for measuring relaxation times, Rev. Sci. Instrum. 29 (1958) 688–691.

[21] H.W. Weber, R. Kimmich, Anomalous segment diffusion in polymers and NMR relaxation spectroscopy, Macromolecules 26 (1993) 2597–2606.

[22] A. Schallamach, The heat conductivity of rubber at low temperatures, Proc. Phys. Soc. 53 (1941) 214–218.

[23] N. Bekkedahl, H. Matheson, Heat capacity, entropy and free-energy of rubber hydrocarbon, J. Res. Nation Bur. Stand. 15 (1935) 503.